



UNICA

UNIVERSITÀ
DEGLI STUDI
DI CAGLIARI



Università di Cagliari

UNICA IRIS Institutional Research Information System

This is the Author's manuscript version of the following contribution:

F. dell'Isola, V.A. Eremeyev, V.A. Korolenko, Y.O. Solyaev, Deformation of an elastic second gradient spherical body under equatorial line density of dead forces, European Journal of Mechanics - A/Solids, Volume 103, 2024, 105153, ISSN 0997-7538,

(<https://www.sciencedirect.com/science/article/pii/S0997753823002450>)

The publisher's version is available at:

<https://doi.org/10.1016/j.euromechsol.2023.105153>.

When citing, please refer to the published version.

Deformation of an elastic second gradient spherical body under equatorial line density of dead forces

F. Dell'Isola, V. A. Eremeyev, V. Korolenko, Y. Solyaev

October 9, 2023

Abstract

We consider a body having, in the reference configuration, a spherical shape. We assume that the deformation energy of this body depends on the first and second gradient of displacement and we consider an equatorial line density of dead loads: that is forces per unit line directed in radial direction applied in the equator of the sphere. We limit our analysis to the case of linearised second isotropic elasticity (for which the more general energy was determined by Mindlin) with only one characteristic length. Differently to what happens in first gradient continua, we show that already for the particular class second gradient continua considered these forces do not determine infinite displacements in the direction of applied field of dead line forces. Instead we show, by using a series method for the solution of the considered elastic problem, that the displacements are finite and that in the current configuration there is not the formation of an edge at the material points where the forces are applied. Further investigations are therefore needed for establishing if this elastic-regime edge formation is made possible: I) either in the case of more general linear elastic constitutive equations or II) only when large deformations are considered or III) if non-elastic phenomena are involved.

Keywords: Strain gradient elasticity, Line loads, Stress concentration, Smoothed solution

1 Introduction

Second gradient continua have the capacity of supporting contact forces concentrated on edges(see e.g. [1–7]). It has been recently recognised that externally applied Eulerian double forces once transported in the reference configuration can produce Lagrangian edge forces (see [8]). It is therefore interesting to try to investigate if forces per unit line, applied on regular surfaces may produce edges in the Eulerian configuration.

In the present paper we prove that in the case of a particular simplified class of second gradient materials with only one characteristic length and in the

hypothesis of small deformations (i.e. linearised case) the application of line forces does not produce new edges in the current configuration. More precisely, based on the results by Mindlin, we start by considering a deformable second gradient homogeneous isotropic body that, in the reference configuration, has a spherical shape: the considered deformation energy depends on the first and second gradient of displacement, is quadratic and has the form given by equation (1) in the particular case specified by equation (6). We assume that an equatorial line density of external dead loads is applied to considered a body such that the applied force distribution per unit line is concentrated on the equator of the sphere and that it is directed in the radial direction.

This linear elastic problem has been studied (see [9–11]) in the case of isotropic first gradient homogeneous spherical bodies: the displacement field, in this case, is infinite in the circle where the forces are applied. This apparently paradoxical situation is often explained (in our opinion in a completely inconsistent way) by stating that: "in physical situations there is not such a thing as a line concentrated force". This apparent paradox is solved by stating that: "the only applicable forces are forces per unit area and a line force is nothing else than a surface distributed force applied on a very narrow stripe". Consequently the problem which is studied (see [9]) is the problem of deformation of a sphere on which a dead load is applied in a "stripe of parallels" of small thickness. It is then observed that the narrower the stripe the larger is the equatorial displacement and that when the stripe thickness tends to zero this displacement diverges together with strain. Obviously this result, a posteriori, excludes the possibility itself of using linearised models. In our opinion this apparent paradox can be simply interpreted as follows: when one needs to model external loads as forces per unit line, then first gradient models are not applicable, at least in the vicinity of the curve where external loads are applied. The modelling possibility which we explore in this paper is the following: When one wants to consider external applied forces concentrated on lines, are second gradient continuum models capable to predict finite displacements of the material points where the loads are applied?

We prove that, differently from what happens in first gradient continua, for the particular class second gradient continua considered in equations (1) and (6) the answer to the previous question is: yes! The apparent paradox described before does not occur in second gradient continua! Another natural question arises: Are forces per unit line capable to determine, in the regime of linear elasticity, the formation of new edges, that is edge in the Eulerian configuration?

To answer to both questions we: i) use Papkovitch-Neuber general solution via potentials of the PDE for displacement field characterising equilibrium configurations [12–14], ii) represent the introduced potentials via a series representation in spherical coordinates, iii) impose the applied dead loads representing in series the Dirac delta distribution having as variable the "latitude" angle.

Then we manage to evaluate numerically the calculated series and we observe that: i) the equilibrium displacements under applied loads are finite and ii) in the current configuration no edges (i.e. no jumps of the normals to the current

body surface) are formed in the curve occupied by the material points on which line forces are applied.

Albeit interesting, the presented results do not completely answer to the problem of elastic edge formation. Clearly further investigations are therefore to answer to the question concerning the possibility of Eulerian edges formations, induced by line forces, in the elastic regime. Is this elastic formation possible? For obtaining it do we need more general linear elastic constitutive equations? Or do we need to consider large elastic deformations regimes (i.e. non-linear constitutive equations)? In case that all previous questions will have negative answers one could be led to conclude that inelastic models are the only ones in which Eulerian edge formation is possible.

2 Strain gradient elasticity theory (SGET)

We consider an isotropic strain gradient elasticity theory according to Mindlin Form II, in which the strain energy density depends on strain and gradient of strain [15]:

$$U(\boldsymbol{\varepsilon}, \nabla \boldsymbol{\varepsilon}) = \frac{1}{2} \boldsymbol{\varepsilon} : \mathbf{C} : \boldsymbol{\varepsilon} + \frac{1}{2} \nabla \boldsymbol{\varepsilon} : \mathbf{A} : \nabla \boldsymbol{\varepsilon} \quad (1)$$

where \mathbf{C} and \mathbf{A} are the fourth- and sixth-order tensors of the elastic moduli; ∇ is nabla operator; and infinitesimal strain tensor is given by

$$\boldsymbol{\varepsilon} = \frac{1}{2} (\nabla \mathbf{u} + (\nabla \mathbf{u})^T) \quad (2)$$

Constitutive equations are defined for the second-order stress tensor $\boldsymbol{\tau}$ and for the third-order double-stress tensor $\boldsymbol{\mu}$:

$$\boldsymbol{\tau} = \frac{\partial U}{\partial \boldsymbol{\varepsilon}} = \mathbf{C} : \boldsymbol{\varepsilon}, \quad \boldsymbol{\mu} = \frac{\partial U}{\partial \nabla \boldsymbol{\varepsilon}} = \mathbf{A} : \nabla \boldsymbol{\varepsilon} \quad (3)$$

2.1 Constitutive equations

Components of the constitutive tensors \mathbf{C} and \mathbf{A} within the general formulation of Mindlin Form II can be represented as follows [15, 16]:

$$C_{ijkl} = C_{jikl} = C_{ijlk} = C_{klij} = \lambda \delta_{ij} \delta_{kl} + \mu (\delta_{ik} \delta_{jl} + \delta_{il} \delta_{jk}) \quad (4)$$

$$\begin{aligned} A_{ijklmn} &= A_{jiklmn} = A_{ijkmln} = A_{lmnijk} \\ &= a_1 (\delta_{ij} \delta_{kl} \delta_{mn} + \delta_{in} \delta_{jk} \delta_{lm} + \delta_{ij} \delta_{km} \delta_{ln} + \delta_{ik} \delta_{jn} \delta_{lm}) \\ &\quad + a_2 \delta_{ij} \delta_{kn} \delta_{lm} \\ &\quad + a_3 (\delta_{ik} \delta_{jl} \delta_{mn} + \delta_{im} \delta_{jk} \delta_{ln} + \delta_{ik} \delta_{jm} \delta_{ln} + \delta_{il} \delta_{jk} \delta_{mn}) \\ &\quad + a_4 (\delta_{il} \delta_{jm} \delta_{kn} + \delta_{im} \delta_{jl} \delta_{kn}) \\ &\quad + a_5 (\delta_{il} \delta_{jn} \delta_{km} + \delta_{im} \delta_{jn} \delta_{kl} + \delta_{in} \delta_{jl} \delta_{km} + \delta_{in} \delta_{jm} \delta_{kl}) \end{aligned} \quad (5)$$

where λ , μ are the Láme parameters and a_i ($i = 1..5$) are the additional material constants of SGET.

In the following we will consider a simplified theory assuming that $a_1 = a_3 = a_5 = 0$, $a_2 = \ell^2\lambda$, $a_4 = \ell^2\mu$ (ℓ is single length scale parameter [17]) so that six-order tensor (5) takes the form:

$$\begin{aligned} A_{ijklmn} &= A_{jiklmn} = A_{ijkmln} = A_{lmnijk} \\ &= \ell^2 C_{ijlm} \delta_{kn} = \ell^2 (\lambda \delta_{ij} \delta_{lm} \delta_{kn} + \mu (\delta_{il} \delta_{jm} \delta_{kn} + \delta_{im} \delta_{jl} \delta_{kn})) \end{aligned} \quad (6)$$

and the components of stress $\boldsymbol{\tau}$ and double stress $\boldsymbol{\mu}$ (3) become:

$$\begin{aligned} \tau_{ij} &= \tau_{ji} = \lambda \delta_{ij} \varepsilon_{ll} + 2\mu \varepsilon_{ij}, \\ \text{i.e. } \boldsymbol{\tau} &= \lambda \mathbf{I} \nabla \cdot \mathbf{u} + 2\mu \boldsymbol{\varepsilon} \end{aligned} \quad (7)$$

$$\begin{aligned} \mu_{ijk} &= \mu_{jik} = \tau_{ij,k} = \ell^2 (\lambda \delta_{ij} \varepsilon_{ll,k} + 2\mu \varepsilon_{ij,k}), \\ \text{i.e. } \boldsymbol{\mu} &= \ell^2 \nabla \boldsymbol{\tau} = \ell^2 (\lambda \mathbf{I} \nabla \nabla \cdot \mathbf{u} + 2\mu \nabla \boldsymbol{\varepsilon}) \end{aligned} \quad (8)$$

where $\varepsilon_{ij} = \varepsilon_{ji}$ are the components of strain tensor, $\varepsilon_{ij,k}$ are the components of the strain gradient tensor; and repeated indexes imply summation.

2.2 Boundary value problem

The formulation of boundary value problem of SGET can be obtained by using variational approach. In absence of body force it can be stated as follows [15, 18]:

$$\begin{cases} \nabla \cdot \boldsymbol{\sigma} = 0, & \mathbf{r} \in \Omega \\ \mathbf{t} = \bar{\mathbf{t}}, \text{ or } \mathbf{u} = \bar{\mathbf{u}}_s, & \mathbf{r} \in \partial\Omega \\ \mathbf{m} = \bar{\mathbf{m}} \text{ or } \partial_n \mathbf{u} = \bar{\mathbf{g}}, & \mathbf{r} \in \partial\Omega \\ \mathbf{s} = \bar{\mathbf{s}} \text{ or } \mathbf{u} = \bar{\mathbf{u}}_e, & \mathbf{r} \in \partial\partial\Omega \end{cases} \quad (9)$$

where Ω , $\partial\Omega$, $\partial\partial\Omega$ are the body volume and its surface and edges under consideration; \mathbf{r} is the position vector; and the total stress tensor $\boldsymbol{\sigma}$, the surface traction vector \mathbf{t} , the surface double traction vector \mathbf{m} and the edge traction vector \mathbf{s} are given by:

$$\boldsymbol{\sigma} = \boldsymbol{\tau} - \nabla \cdot \boldsymbol{\mu} \quad (10)$$

$$\mathbf{t} = \mathbf{n} \cdot \boldsymbol{\sigma} - \nabla_S \cdot (\mathbf{n} \cdot \boldsymbol{\mu}) - 2H\mathbf{m} \quad (11)$$

$$\mathbf{m} = (\mathbf{n} \otimes \mathbf{n}) : \boldsymbol{\mu} \quad (12)$$

$$\mathbf{s} = [(\mathbf{n} \otimes \boldsymbol{\nu}) : \boldsymbol{\mu}] \quad (13)$$

where $\nabla_S = \nabla - \mathbf{n} \partial_n$ is the surface gradient operator; $H = -\frac{1}{2} \nabla_S \cdot \mathbf{n}$ is the mean curvature; \mathbf{n} is unit outward normal vector on $\partial\Omega$; $\boldsymbol{\nu} = \mathbf{n} \times \mathbf{v}$ and \mathbf{v} are the unit co-normal and tangent vectors to given edge $\partial\partial\Omega$, respectively.

2.3 Papkovitch-Neuber general solution

Substituting (2) into (7), (8) and the result into (9)₁, one can obtain the equilibrium equations of SGET in terms of displacements in the following form [15]:

$$(\lambda + 2\mu)(1 - l_1^2 \nabla^2) \nabla \nabla \cdot \mathbf{u} - \mu(1 - l_2^2 \nabla^2) \nabla \times \nabla \times \mathbf{u} = 0 \quad (14)$$

where $l_1^2 = \frac{4a_1 + a_2 + 4a_3 + 2a_4 + 4a_5}{\lambda + 2\mu}$ and $l_2^2 = \frac{a_3 + a_4 + a_5}{\mu}$ are two length scale parameters that persist in equilibrium equations of general SGET [15, 19], while in the considered simplified theory (6) it is valid that $l_1 = l_2 = l$.

General solution for equilibrium equations (14) in absence of body forces can be represented in the following form [13, 14]:

$$\begin{aligned} \mathbf{u} &= \mathbf{u}_c + \mathbf{u}_g, \\ \mathbf{u}_c &= 4(1 - \nu)\mathbf{\Phi} - \nabla(\mathbf{r} \cdot \mathbf{\Phi} + \varphi), \\ \mathbf{u}_g &= \mathbf{\Psi} + \nabla\psi \end{aligned} \quad (15)$$

where ν is the Poisson ratio; and stress functions have to satisfy the Laplace and modified Helmholtz equations as follows:

$$\begin{aligned} \nabla^2 \varphi &= 0, & \nabla^2 \mathbf{\Phi} &= 0, \\ \psi - \ell_1^2 \nabla^2 \psi &= 0, & \mathbf{\Psi} - \ell_2^2 \nabla^2 \mathbf{\Psi} &= 0, & \nabla \cdot \mathbf{\Psi} &= 0 \end{aligned} \quad (16)$$

In the considered representation (15), we have additive decomposition of the displacement field into the so-called classical part (\mathbf{u}_c) and gradient part (\mathbf{u}_g). For the classical part we use standard Papkovitch-Neuber representation [20] with harmonic scalar (ϕ) and vector ($\mathbf{\Phi}$) stress functions. Gradient part of displacement field is also represented via scalar (ψ) and divergence free vector ($\mathbf{\Psi}$) stress functions that obey the modified Helmholtz equations with the length scale parameters l_1 and l_2 , respectively. Notably, that in the case of considered simplified theory (6) the representation of gradient part \mathbf{u}_g is reduced to the standard Helmholtz decomposition. The representation (15) has been suggested in Ref. [13] and its formal derivation together with the variant of the proof for its completeness has been established in Ref. [14]. Other variants of definitions for the Papkovitch-Neuber solution within SGET has been considered in Refs. [12, 15, 21–24].

Notably, that for the orthogonal curvilinear coordinates we can represent the solenoidal field $\mathbf{\Psi}(\mathbf{r})$ that obeys the modified vector Helmholtz equation via two scalar functions that obey the scalar Helmholtz equations [25]. Namely, for the spherical coordinate system, the following representation is valid:

$$\begin{aligned} \mathbf{\Psi} &= \nabla \times (r \bar{\chi} \mathbf{e}_r) + \nabla \times \nabla \times (r \chi \mathbf{e}_r) \\ \bar{\chi} - \ell_2^2 \nabla^2 \bar{\chi} &= 0, & \chi - \ell_2^2 \nabla^2 \chi &= 0 \end{aligned} \quad (17)$$

where, $\bar{\chi}(\mathbf{r})$ defines the anti-plane deformations and $\chi(\mathbf{r})$ defines the in-plane deformations, $r = |\mathbf{r}|$ is radial distance and \mathbf{e}_r is unit vector along radial direction.

Presented form of Papkovitch-Neuber general solution (15) and the representation of additional vector stress function via scalars (17) greatly simplifies analytical solutions of particular boundary value problems in spherical coordinates. Similar definitions (17) can be obtained for the other curvilinear coordinates that allow separation of variables for Helmholtz vector equation [25].

3 Sphere under equatorial load: series solution

Let us consider a spherical body Ω of radius r_0 under axisymmetric loading conditions. It is convenient to use then the spherical coordinate system $\mathbf{r} = r\mathbf{e}_r + \theta\mathbf{e}_\theta + \phi\mathbf{e}_\phi$ ($r \geq 0$, $0 \leq \theta \leq \pi$, $0 \leq \phi < 2\pi$), for which the axis of symmetry is defined by the polar angles $\theta = 0$, $\theta = \pi$. Displacement field and stress functions are assumed to be independent on azimuthal angle (ϕ) and their corresponding azimuthal components are zero:

$$\begin{aligned} \mathbf{u}(r, \theta) &= u_r \mathbf{e}_r + u_\theta \mathbf{e}_\theta, \\ \mathbf{\Phi}(r, \theta) &= \Phi_r \mathbf{e}_r + \Phi_\theta \mathbf{e}_\theta, \\ \mathbf{\Psi}(r, \theta) &= \Psi_r \mathbf{e}_r + \Psi_\theta \mathbf{e}_\theta = \nabla \times \nabla \times (r \mathbf{e}_r \chi(r, \theta)), \\ &\implies \Psi_r = -\frac{\cot \theta}{r} \frac{\partial \chi}{\partial \theta} - \frac{1}{r} \frac{\partial^2 \chi}{\partial \theta^2}, \quad \Psi_\theta = \frac{1}{r} \frac{\partial \chi}{\partial \theta} + \frac{\partial^2 \chi}{\partial r \partial \theta} \end{aligned} \quad (18)$$

where we use the definition for nabla operator for axisymmetric problems $\nabla = \left\{ \frac{\partial}{\partial r}, \frac{1}{r} \frac{\partial}{\partial \theta}, 0 \right\}$ and take into account that there will be no anti-plane deformations (no torsion) so that $\bar{\chi} \equiv 0$.

Combining (18) and (15) we can obtain the following representation for the displacement field:

$$\begin{aligned} u_r &= 4(1-\nu)\Phi_r - \frac{\partial}{\partial r} \left(r\Phi_r + \varphi + \psi \right) - \frac{\cot \theta}{r} \frac{\partial \chi}{\partial \theta} - \frac{1}{r} \frac{\partial^2 \chi}{\partial \theta^2} \\ u_\theta &= 4(1-\nu)\Phi_\theta - \frac{1}{r} \frac{\partial}{\partial \theta} \left(r\Phi_r + \varphi + \psi \right) + \frac{1}{r} \frac{\partial \chi}{\partial \theta} + \frac{\partial^2 \chi}{\partial r \partial \theta} \end{aligned} \quad (19)$$

where harmonic stress functions $\mathbf{\Phi}(r, \theta)$ and $\varphi(r, \theta)$ for the interior domains can be defined as follows [20]:

$$\begin{aligned} \Phi_r &= - \sum_{n=0}^{\infty} A_n (n+1) r^{n+1} P_n(\cos \theta) \\ \Phi_\theta &= \sum_{n=0}^{\infty} A_n r^{n+1} \frac{\partial P_n(\cos \theta)}{\partial \theta} \\ \varphi &= - \sum_{n=0}^{\infty} B_n r^n P_n(\cos \theta) \end{aligned} \quad (20)$$

where $P_n(\dots)$ are the Legendre polynomials.

Additional stress functions of gradient theory $\psi(r, \theta)$ and $\chi(r, \theta)$ that obey the modified Helmholtz equations can be expressed as follows [26]:

$$\begin{aligned}
\psi &= \sum_{n=0}^{\infty} C_n i_n\left(\frac{r}{l_1}\right) P_n(\cos \theta) \\
\chi &= \sum_{n=0}^{\infty} D_n i_n\left(\frac{r}{l_2}\right) P_n(\cos \theta)
\end{aligned} \tag{21}$$

where $i_n(\dots)$ is the modified spherical Bessel function of the first kind that is bounded in the interior domain.

Note that series representation of the stress functions (20), (21) are complete in a Trefftz sense [26, 27], i.e. they allow to obtain all kind of solutions for the corresponding governing equations (16). Coefficients B_0 and D_0 in (20), (21) can be neglected since they will not arise in the displacement solution (19). Coefficient B_1 corresponds to the rigid body displacement along symmetry axis and can be also neglected [20].

Non-zero components of traction (11) and double traction (12) on the sphere surface ($r = r_0$, $\mathbf{n} = \mathbf{e}_r$) that are involved in the axisymmetric problems in spherical coordinates are the following:

$$\begin{aligned}
\mathbf{t} &= \mathbf{n} \cdot (\boldsymbol{\tau} - \nabla \cdot \boldsymbol{\mu}) - \nabla_S \cdot (\mathbf{n} \cdot \boldsymbol{\mu}), \quad \text{i.e.} \\
t_r &= \tau_{rr} - \frac{\partial \mu_{rrr}}{\partial r} - \frac{\partial \mu_{rr\theta}}{\partial \theta} - \frac{\partial \mu_{r\theta r}}{\partial \theta} - 4\mu_{rrr} + 3\mu_{r\theta\theta} \\
&\quad + \mu_{\theta\theta r} + \mu_{\phi\phi r} + 3\mu_{r\phi\phi} - (\mu_{rr\theta} + \mu_{r\theta r}) \cot \theta \\
t_\theta &= \tau_{r\theta} - \frac{\partial \mu_{r\theta r}}{\partial r} - \frac{\partial \mu_{r\theta\theta}}{\partial \theta} - \frac{\partial \mu_{\theta\theta r}}{\partial \theta} - 5\mu_{r\theta r} - \mu_{rr\theta} + 2\mu_{\theta\theta\theta} \\
&\quad + 2\mu_{\theta\phi\phi} + (\mu_{\phi\phi r} + \mu_{r\phi\phi} - \mu_{r\theta\theta} - \mu_{\theta\theta r}) \cot \theta
\end{aligned} \tag{22}$$

$$\begin{aligned}
\mathbf{m} &= (\mathbf{n} \otimes \mathbf{n}) : \boldsymbol{\mu}, \quad \text{i.e.} \\
m_r &= \mu_{rrr}, \quad m_\theta = \mu_{\theta rr}
\end{aligned} \tag{23}$$

where we take into account that the condition of zero double-tractions will be implied in the considered problems ($\bar{\mathbf{m}} = 0$) and the following components of the double stress tensor should be identically zero within the axisymmetric problems of simplified SGET:

$$\mu_{rr\phi} = \mu_{r\theta\phi} = \mu_{r\phi r} = \mu_{r\phi\theta} = \mu_{\theta\theta\phi} = \mu_{\theta\phi\theta} = \mu_{\theta\phi r} = \mu_{\phi\phi\phi} = 0 \tag{24}$$

3.1 Loading conditions: Dirac delta function

Loading conditions at the surface of sphere ($r = r_0$) is imposed according to classical definition of traction for the problem of sphere under equatorial line load [20] together with additional SGET conditions for zero double-tractions:

$$r = r_0 : \quad \bar{\mathbf{t}} = -q \delta\left(\theta - \frac{\pi}{2}\right) \mathbf{e}_r, \quad \bar{\mathbf{m}} = \mathbf{0} \tag{25}$$

where $\delta(\dots)$ is Dirac delta function and q is the compressive force per unit line distributed over equator of sphere ($\theta = \pi/2$), see Fig. 1a.

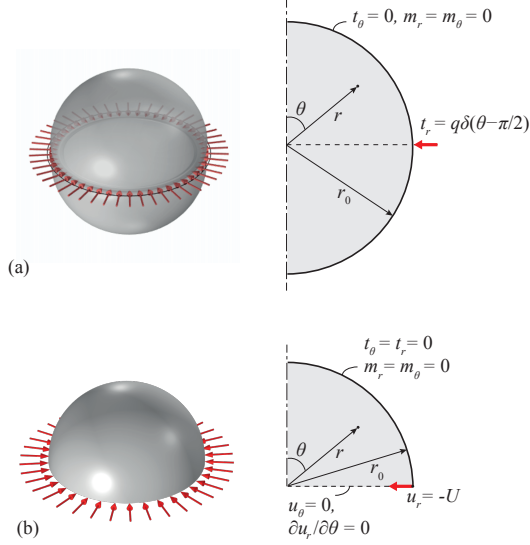


Figure 1: Sphere under equatorial line load. Illustrations for the statement with the full sphere (a) and for the statement with the half sphere accounting for the symmetry (b)

Taking into account definitions for tractions and double-tractions (22), (23) we obtain the following four independent boundary conditions:

$$t_r = -q \delta(\theta - \frac{\pi}{2}), \quad t_\theta = 0, \quad m_r = 0, \quad m_\theta = 0 \quad (26)$$

To find the solution, Dirac delta function should be also expressed in terms of spherical harmonics [11]:

$$\delta(\theta - \frac{\pi}{2}) = \sum_{n=0}^{\infty} \frac{2n+1}{2} P_n(0) P_n(\cos \theta), \quad (27)$$

$$P_n(0) = \begin{cases} \frac{(-1)^n (2n)!}{2^{2n} (n!)^2}, & n = 2k, (k = 0, 1, 2, \dots) \\ 0, & \text{otherwise} \end{cases}$$

Solution of the problem is found then by using standard algorithm. We choose the maximum number of terms in series representation $n = N$ and use (20), (21) to define displacement field (19). Then we find strain $\boldsymbol{\varepsilon}$ (2), Cauchy stress $\boldsymbol{\tau}$ (7) and double stress $\boldsymbol{\mu}$ (8). Then we use the boundary conditions for traction and double traction (26) with series representation of the load (27) to obtain $4(N+1)$ linear equations with respect to A_n, B_n, C_n, D_n ($n = 0 \dots N$) that corresponds to different terms in the series of spherical harmonics. Solution of this system provide us the values of unknown constants of the series. Increasing the number of terms in series N we can evaluate the convergence of the solution.

3.2 Loading condition: edge traction on a half-sphere

Another approach to the solution of the problem can be realized if one takes into account the symmetry of the problem and consider only the half of the sphere (Fig. 1b). In this case we have a plane of symmetry and additional circular edge, which can be used for definition of the edge-type boundary condition within SGET (see (9), (13)).

At the plane of symmetry ($\theta = \pi/2$) the generalized symmetry boundary conditions should be prescribed:

$$\begin{aligned} \mathbf{u} \cdot \mathbf{n} = 0 & \implies u_\theta = 0 \\ \partial_n \mathbf{u} \cdot (\mathbf{I} - \mathbf{n} \otimes \mathbf{n}) = 0 & \implies \frac{\partial u_r}{\partial \theta} = 0 \quad \left(\text{and } \frac{\partial u_\phi}{\partial \theta} \equiv 0 \right) \end{aligned} \quad (28)$$

where $\mathbf{n} = \mathbf{e}_\theta$ at the plane of symmetry; and the second condition for gradient of displacement means the absence of shear and rotations at the plane of symmetry.

Boundary conditions at the external surface of sphere ($r = r_0$) become:

$$\bar{\mathbf{t}} = \mathbf{0}, \quad \bar{\mathbf{m}} = \mathbf{0} \quad (29)$$

At the circular edge of a half-sphere ($\theta = \pi/2, r = r_0$) we can explicitly define the following kinematic (essential) boundary condition:

$$\bar{\mathbf{u}}_e = -U \mathbf{e}_r, \quad \text{i.e. } u_r = U, u_\theta = 0, u_\phi = 0 \quad (30)$$

Notably, that two conditions for the angular displacements in (30) are already satisfied by the imposed conditions of axial symmetry ($u_\phi = 0$, see (18)) and plane of symmetry ($u_\theta = 0$, see (28)). Therefore, under kinematic type of loading we have single additional boundary condition at the edge:

$$\theta = \pi/2, r = r_0 : \quad u_r = -U \quad (31)$$

Solution of the problem for a half-sphere can be found in the following way. At first, both conditions for the plane of symmetry (28) will be satisfied identically if one use only the terms with numbers $n = 2k$ ($k = 0, 1, 2, \dots, N$) in series (20), (21). Secondly, traction-free boundary conditions (29) give us $4(N + 1)$ equations to found unknown constants A_n, B_n, C_n, D_n in series (20), (21) (similarly to the problem with full sphere). Thus, within the considered representation of stress functions (20), (21) we do not have enough variables to satisfy additional edge-type boundary condition (31). Nevertheless, the representation for the displacement field or for the stress functions can be extended by any kind of particular solution¹ that obeys the prescribed equilibrium equation (for the displacement) or the potential equations (16) (for the stress functions).

¹Although the representations of the harmonic and Helmholtz-type stress functions through the series of spherical harmonics (20), (21) are complete, for the particular problems it can be useful to introduce additional particular solutions that corresponds to the considered special type of the boundary conditions [27].

For the classical elasticity problem it is known that the following particular solution for the displacement field can be extracted from the full series representation of the solution [20]:

$$\begin{aligned}
\mathbf{u}_c^* &= u_r^{(c)} \mathbf{e}_r + u_\theta^{(c)} \mathbf{e}_\theta, \\
u_r^{(c)} &= Q \frac{1}{8\mu\bar{r}s_1} \left((1 - \bar{r}^2) \left((1 - \bar{r}^2) \frac{2E(k)}{\pi s_2^2} - s_1 \right) + 4(1 - \nu)(1 + \bar{r}^2) \left(\frac{2K(k)}{\pi} - s_1 \right) \right) \\
u_\theta^{(c)} &= -Q \frac{1 - \bar{r}^2}{4\mu s_1} \cos \theta \left(\frac{2E(k)}{\pi s_2^2} - \frac{4}{\pi(s_1^2 - s_2^2)} \left(\frac{s_1^2}{s_2^2} E(k) - K(k) \right) \right)
\end{aligned} \tag{32}$$

where $\bar{r} = r/r_0$ is normalized radial coordinate; $K(k)$ and $E(k)$ are the complete elliptic integrals of the first and second kind, respectively; $s_{1,2} = \sqrt{1 + \bar{r}^2 \pm 2\bar{r} \sin \theta}$, $k = \sqrt{(s_1^2 - s_2^2)/s_1^2}$; and Q is some unknown coefficient that should be found from the solution (within classical elasticity this coefficient equals to the line load q).

Note, that particular solution (32) describe the singular behaviour of the solution around the loaded equator within the classical elasticity. Namely, it can be shown that this solution contains logarithmic singularity for the radial displacement $u_r^{(c)}$ and discontinuity of the angular displacements $u_\theta^{(c)}$ at the equator $\theta = \pi/2$.

Within SGET, one should find the gradient counterpart \mathbf{u}_g^* of the classical particular solution (32) so that the total particular solution can be presented as the sum $\mathbf{u}^* = \mathbf{u}_c^* + \mathbf{u}_g^*$ and satisfies the high-order equilibrium equations of the theory (14). Then, one should add this particular solution to the representation for the displacement field (15). In such a way, in this representation one will obtain additional constant Q that corresponds to the behavior of the solution around the loaded equator and can be used to satisfy edge-type boundary condition (31). Similar analysis with the particular solutions for the problem of the wedge under concentrated load have been presented in Ref. [13]. In this plane problem for the wedge, the particular classical and gradient solutions become rather simple and can be found in compact analytical form.

In the present case of 3D problem for sphere, classical particular solution (32) takes rather complicated form and there is no straightforward way for derivation of its gradient counterpart. Thus, in the present study the statement with a half sphere will be not considered in the numerical analysis. Nevertheless, we can obtain three important consequence from the statement of this problem:

1. Standard algorithm (when the number of constants in series solution (20), (21) for each spherical harmonic equals to the number of boundary conditions (26)) is not applicable for the problems with edge type boundary conditions within SGET.
2. SGET allows do define the finite value of the displacement at the equator of sphere (31), that cannot be done within classical theory.
3. The generalized symmetry conditions (28) for the normal gradients of displacement are prescribed explicitly within SGET and, as the result, they

provide smooth distribution of shear, rotations as well as the continuous change of surface normals under the line load.

4 Results of numerical calculations

In the examples of numerical calculations we use the following values of parameters: $E = 1$ GPa, $\nu = 0.25$, $r_0 = 1$ m, $q = 0.001E r_0$. As an example we consider simplified SGET with $l_1 = l_2 = l$.

Convergence analysis of series solution is performed based on four standard criteria. We consider the ratio and the root tests, according to which the series $\sum_{n=1}^{\infty} f_n$ converges if

$$\lim_{n \rightarrow \infty} \rho_1 < 1, \quad \rho_1 = \frac{f_{n+1}}{f_n} \quad (33)$$

or

$$\lim_{n \rightarrow \infty} \rho_2 < 1, \quad \rho_2 = \sqrt[n]{f_n} \quad (34)$$

additionally we will use Raabe's test, which require for the convergence

$$\lim_{n \rightarrow \infty} \rho_3 > 1, \quad \rho_3 = n \left(\frac{f_n}{f_{n+1}} - 1 \right) \quad (35)$$

and Kummer's test:

$$\lim_{n \rightarrow \infty} \rho_4 > 0, \quad \rho_4 = a_n \frac{f_n}{f_{n+1}} - a_{n+1} \quad (36)$$

in which we use $a_n = n \log n$ ($n \geq 1$) such that $\sum_{n=1}^{\infty} a_n^{-1}$ diverges.

Convergence tests were applied to the obtained series solution for the displacements (19) and strains (2) represented via stress functions (20), (21). Coefficients in these series were found from the solution of the problem described in section 3.1. Given relations (33)-(36) imply that series are non-alternating and all terms are positive. This was checked during analysis. In the case when all terms are negative, we can just use their absolute values assuming the change of sign of the applied load.

Convergence analysis was performed for radial displacements and strain at the equator on the sphere surface $r = r_0$, $\theta = \pi/2$ (where the line load is applied). Notably, that within the classical elasticity these quantities have infinite values and corresponding series solution diverges [20]. In the convergence analysis within SGET we used values of the length scale parameter $l = r_0$ (strong gradient effects), $l = r_0/100$ (weak gradient effects), $l = 0$ (classical elasticity divergent solution).

Values of found first 50 non-zero terms and the summed series for $u_r(r_0, \pi/2, 0)$ and $\varepsilon_{rr}(r_0, \pi/2, 0)$ are presented in Figs. 2, 3. Note, that all terms in series solution $u_r^{(n)}$ and $\varepsilon_{rr}^{(n)}$ are negative under prescribed compression line load. In Figs. 2b, 3b it is well seen that the strain gradient solution with $l = r_0$ is convergent, though the difference between the rate of convergence for the gradient solution

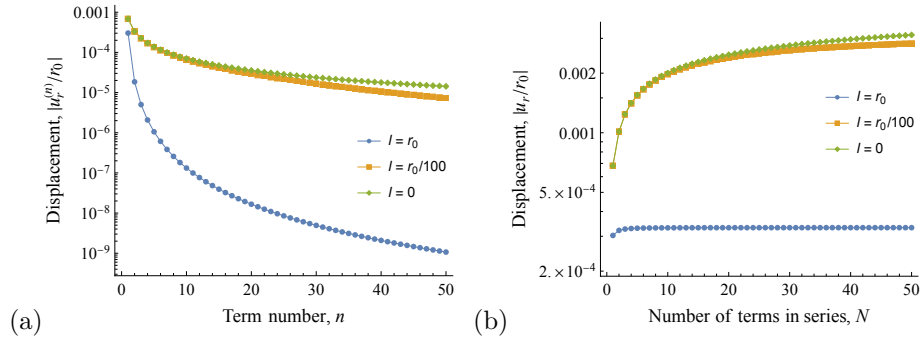


Figure 2: Series solution for radial displacement evaluated at the equator of sphere, (a): numerical values of terms in series solution, (b): Dependence of the solution on the number of terms N

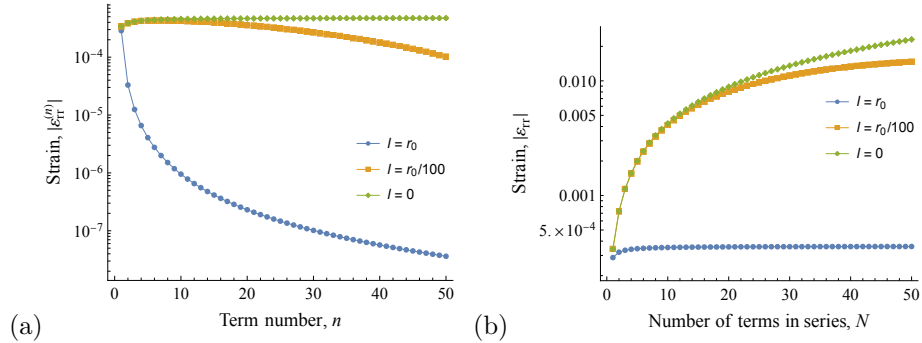


Figure 3: Series solution for radial strain evaluated at equator of sphere, (a): numerical values of terms in series solution, (b): Dependence of series solution on the number of terms N

with $l = r_0/100$ and classical solution (that is known to be divergent) is not well seen. To provide an accurate check of convergence we applied criteria (33)-(36) for evaluated series.

Evaluated convergence criteria are presented in Figs. 4, 5. It is seen that the ratio and the root tests (δ_1 and δ_2) may become inconclusive since they take values close to 1 for the large number of terms N in series solutions (Fig. 4a, b, Fig. 5a, b). The most informative criterion is the Kummer's test (Figs. 4d, 5d), for which within the classical elasticity solution we obtained $\delta_4 < 0$ that confirms the known fact that the classical solution for the considered problem is divergent at equator. In opposite, for the solution of strain gradient elasticity we have $\delta_4 > 0$ (36), so that this solution tend to converge and the bounded values of displacement and strain arise at the equator of sphere under the line load.

The deformed state of sphere found based on series solution with $N = 50$ within SGET is presented in Fig. 6 for different values of the length scale

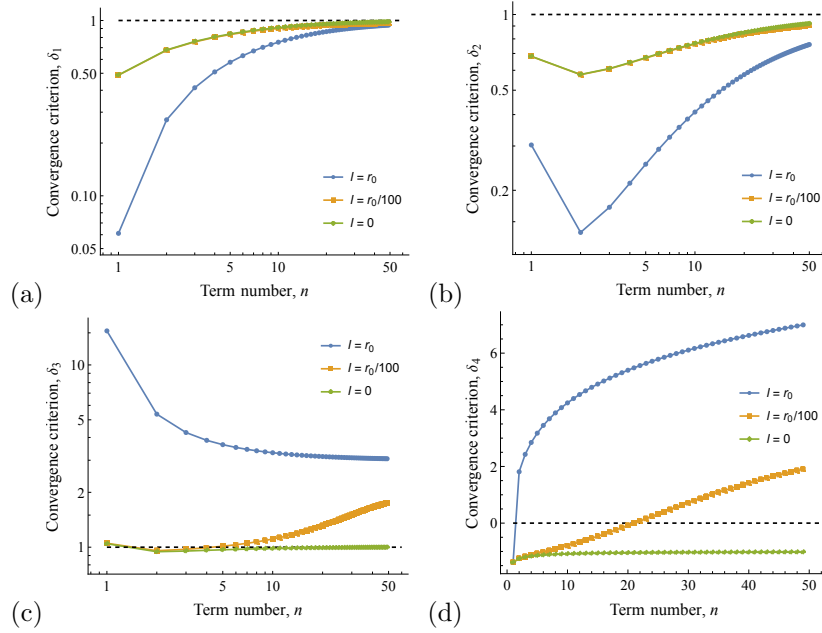


Figure 4: Convergence criteria for series solution for radial displacements $u_r(r_0, \pi/2)$, (a) ratio test, (b) root test, (c) Raabe's test, (d) Kummer's test

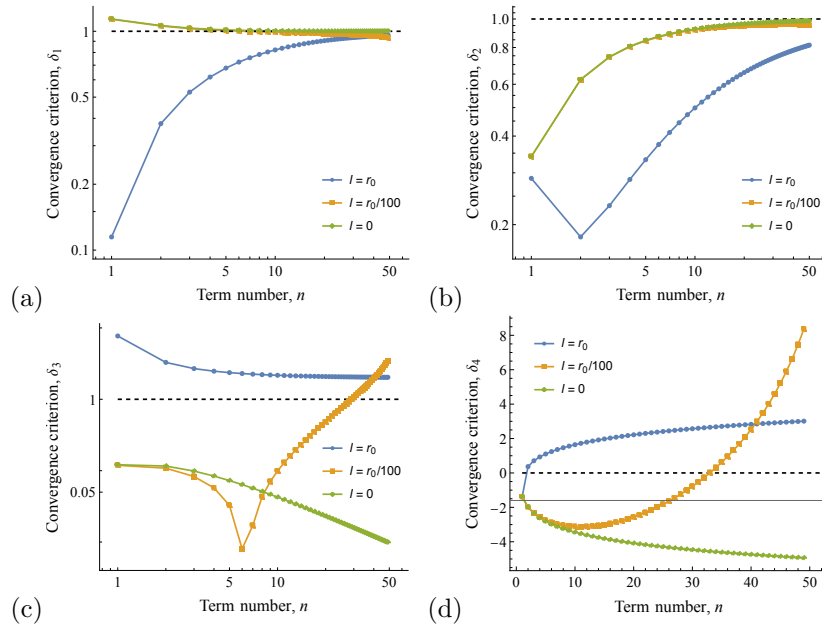


Figure 5: Convergence criteria for series solution for radial strain $\varepsilon_{rr}(r_0, \pi/2)$, (a) ratio test, (b) root test, (c) Raabe's test, (d) Kummer's test

parameter. It is seen that change of the length scale parameter significantly affects only the deformations at equator of sphere where the load is applied. The deformed state is smooth and does not contain non-continuous or non-smooth regions. In more details it is shown in Fig. 7, where we present the distribution of evaluated displacements along the angular coordinate $\theta \in [0, \pi]$ on the surface of sphere. Maximum radial displacements become larger for the smaller length scale parameters though its distribution remains smooth (Fig. 7a). At the poles of sphere there arise some noise in the solution for the smallest length scale parameters (red curve in Fig. 7a) since the convergence become worse and it needs more terms in series.

Angular displacements always have zero values at the equator of sphere, however for the small values of the length scale parameter there arise the regions of the local extremums (red curve in Fig. 7b). Distance between these extremums becomes smaller and their amplitudes become larger for the smaller length scale parameters. As the result, in the limit case of classical elasticity ($l = 0$) there will arise the discontinuity of angular displacement at the equator of sphere. Illustration for such behavior of classical solution is given in Fig. 8 where we show the comparison of SGET solution in the case of smallest considered length scale parameter ($l = 0.01$) (this solution converges very slowly that results in a wavy curves) and classical elasticity solution obtained by using FEM. The last one, obviously, is mesh-dependent around the equator of sphere. This classical FEM solution was obtained by using second-order elements within the linear formulation and with smallest element size equals to $0.0025r_0$. In Fig. 8 it is seen that obtained series solution within SGET in the case of small l tends to classical elasticity solution with singular (mesh-dependent) and non-continuous behavior of the displacement field at equator.

The convergence rate of the solution for the strain field is lower in comparison with those for the displacements. Therefore, to obtain the resulting picture for

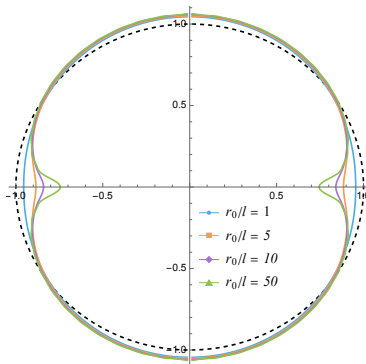


Figure 6: The deformed state of sphere under equatorial load within SGET for different values of the length scale parameter ($r_0 = 1$ m). The scale factor for deformations is 100.

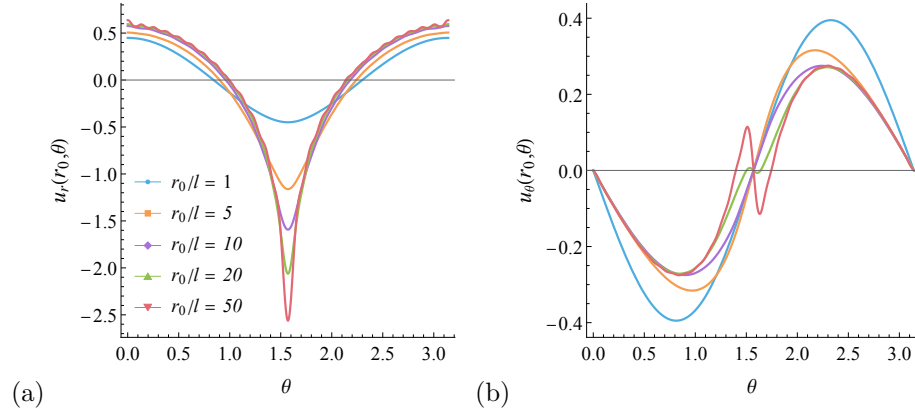


Figure 7: Distribution of radial (a) and angular (b) displacements along angular coordinate on the surface of sphere within SGET solution for different ratio between the sphere radius r_0 and the length scale parameter l .

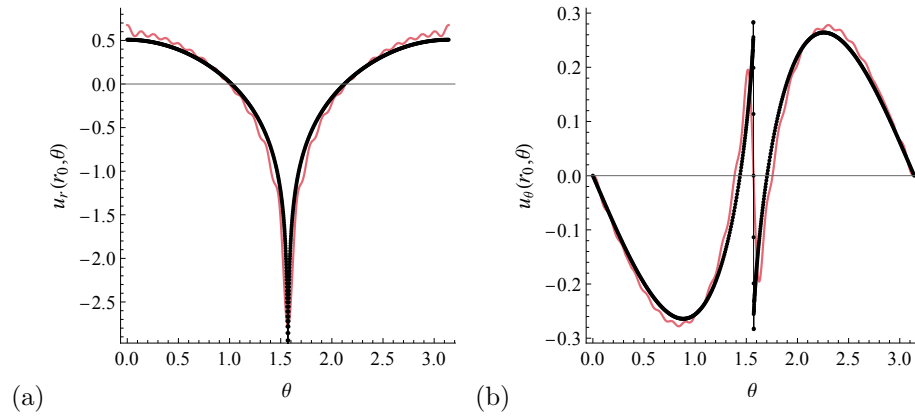


Figure 8: Distribution of radial (a) and angular (b) displacements along angular coordinate on the surface of sphere. SGET solution for $r_0/l = 100$ is shown by red line, classical elasticity FE solution is shown by black points (in FE mesh data points)

the strain field one needs more terms in series and longer calculations. Obtained results for the shear strain distribution along the surface of sphere is shown in Fig. 9. The main result is the obtained continuous distribution of shear strain across equatorial line (at $\theta = \pi/2$). Within classical elasticity at this position there arise discontinuous ($\pm\infty$) shear strain and corresponding discontinuous change of orientation of surface normal. Within SGET we always have zero values of the shear strain at equator and continuous solution with extremums on the both sides from equator. For the smaller values of the length scale parameter these extremums becomes closer and higher and tend to infinity when $l \rightarrow 0$.

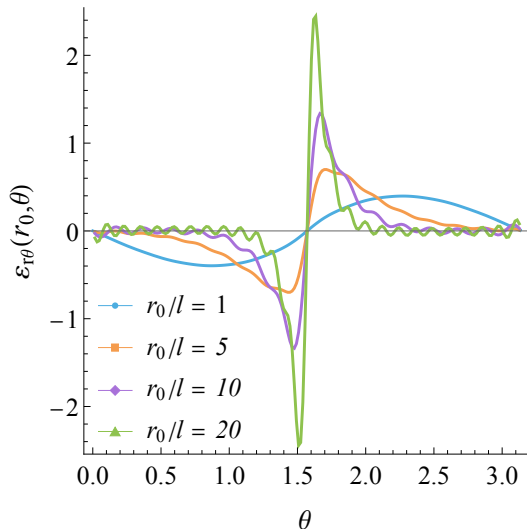


Figure 9: Distribution of shear strain $\varepsilon_{r\theta}$ along angular coordinate on the surface of sphere

5 Conclusions and perspectives

As it is well-known from basic continuum mechanics the normals to surfaces are transported under placement by the Piola Formula [18]. Piola's formula simply implies that the normal of a material surface in Eulerian description depends only on the displacement tangent derivatives in the directions tangent to the surface in the Lagrangian configuration. It is therefore also simple to see that the plots in Figs. 7, 8 imply that, in the hypotheses considered in the present paper, one has the jump of the normals in the current configuration only when the second gradient length-scale tends to zero, so that both the equatorial displacement tends to infinity and the normals in the passage through the equator suffer a jump. We conjecture that also when all the elastic terms in equation (6) will not be considered vanishing the same situation will present itself.

Therefore, the possibilities of elastic formation of edges in the current configuration seem limited to the consideration of the case of either 1) non-isotropic and/non homogeneous materials or 2) non-linear elasticity. We believe that the case of more general isotropic linear second gradient materials can be studied with the methods presented here and a step towards this generalisation must be attempted. It seems also possible, with the classical methods of the theory of elasticity (see e.g. [20]), the study of the deformations produced by double forces concentrated on curves in both the cases of second and third gradient materials. A more drastic change of viewpoint seems necessary to deal with the case of non-linear deformations. Albeit a perturbative Signorini type technique (see e.g. [28]) most likely will be able to produce interesting results, it is clear

that an efficient FE method must be developed for dealing with this case: in this context the results found in the present paper may be of use, by constituting a benchmark for testing such a method.

Acknowledgments

VK and YS acknowledge the Russian Science Foundation grant 23-49-10061 issued to Moscow Aviation Institute.

References

- [1] Paul Germain. The method of virtual power in the mechanics of continuous media, I: Second-gradient theory. *Mathematics and Mechanics of Complex Systems*, 8(2):153–190, 2020.
- [2] Paul Germain. Sur l’application de la méthode des puissances virtuelles en mécanique des milieux continus. *CR Acad. Sci. Paris*, 274:1051–1055, 1972.
- [3] Francesco dell’Isola and Pierre Seppecher. Edge contact forces and quasi-balanced power. *Meccanica*, 32:33–52, 1997.
- [4] Victor A Eremeyev and Francesco dell’Isola. On weak solutions of the boundary value problem within linear dilatational strain gradient elasticity for polyhedral Lipschitz domains. *Mathematics and Mechanics of Solids*, 27(3):433–445, 2022.
- [5] Raymond David Mindlin and N N Eshel. On first strain-gradient theories in linear elasticity. *International Journal of Solids and Structures*, 4(1): 109–124, 1968.
- [6] Raymond David Mindlin. Second gradient of strain and surface-tension in linear elasticity. *International Journal of Solids and Structures*, 1(4): 417–438, 1965.
- [7] Paul Germain. La méthode des puissances virtuelles en mécanique des milieux continus, première partie: théorie du second gradient. *J. Mécanique*, 12(2):235–274, 1973.
- [8] Francesco dell’Isola, Simon R Eugster, Roberto Fedele, and Pierre Seppecher. Second-gradient continua: From Lagrangian to Eulerian and back. *Mathematics and Mechanics of Solids*, 27(12):2715–2750, 2022.
- [9] A I Luri’e. *Three-dimensional problems of the theory of elasticity*. John Wiley, 1964.

- [10] HL Duan, Jianxiang Wang, ZP Huang, and Bhushan Lal Karihaloo. Eshelby formalism for nano-inhomogeneities. *Proceedings of the Royal Society A: Mathematical, Physical and Engineering Sciences*, 461(2062):3335–3353, 2005.
- [11] Robert W Style, Lucio Isa, and Eric R Dufresne. Adsorption of soft particles at fluid interfaces. *Soft Matter*, 11(37):7412–7419, 2015.
- [12] S Lurie, P Belov, D Volkov-Bogorodsky, and N Tuchkova. Interphase layer theory and application in the mechanics of composite materials. *Journal of materials science*, 41:6693–6707, 2006.
- [13] Yury Solyaev, Sergey Lurie, Holm Altenbach, and Francesco dell’Isola. On the elastic wedge problem within simplified and incomplete strain gradient elasticity theories. *International Journal of Solids and Structures*, page 111433, 2022.
- [14] Yury Solyaev. Complete general solutions for equilibrium equations of isotropic strain gradient elasticity. *Submitted, arXiv preprint arXiv:2207.08863*, 2022.
- [15] R. D. Mindlin. Micro-structure in linear elasticity. *Archive for Rational Mechanics and Analysis*, 16(1):51–78, 1964. ISSN 00039527. doi: 10.1007/BF00248490.
- [16] Francesco dell’Isola, Giulio Sciarra, and Stefano Vidoli. Generalized hooke’s law for isotropic second gradient materials. *Proceedings of the Royal Society A: Mathematical, Physical and Engineering Sciences*, 465(2107):2177–2196, 2009.
- [17] Castrenze Polizzotto. A hierarchy of simplified constitutive models within isotropic strain gradient elasticity. *European Journal of Mechanics-A/Solids*, 61:92–109, 2017.
- [18] N Auffray, F dell’Isola, V A Eremeyev, A Madeo, and G Rosi. Analytical continuum mechanics ‘a la Hamilton–Piola least action principle for second gradient continua and capillary fluids. *Mathematics and Mechanics of Solids*, 20(4):375–417, 2015.
- [19] Victor A Eremeyev and Markus Lazar. Strong ellipticity within the toupin–mindlin first strain gradient elasticity theory. *Mechanics Research Communications*, 124:103944, 2022.
- [20] A I Lurie. Spatial problems of the theory of elasticity. *Moscow, State Techn. Publishers*, 1955.
- [21] Sergey Lurie, Dmitrii Volkov-Bogorodsky, Anatolii Leontiev, and Elias Aifantis. Eshelby’s inclusion problem in the gradient theory of elasticity: applications to composite materials. *International Journal of Engineering Science*, 49(12):1517–1525, 2011.

- [22] Sergei Khakalo and Jarkko Niiranen. Gradient-elastic stress analysis near cylindrical holes in a plane under bi-axial tension fields. *International Journal of Solids and Structures*, 110:351–366, 2017.
- [23] Yury Solyaev, Sergey Lurie, and Vladimir Korolenko. Three-phase model of particulate composites in second gradient elasticity. *European Journal of Mechanics-A/Solids*, 78:103853, 2019.
- [24] Antonios Charalambopoulos, Theodore Gortsas, and Demosthenes Polyzos. On representing strain gradient elastic solutions of boundary value problems by encompassing the classical elastic solution. *Mathematics*, 10(7):1152, 2022.
- [25] P.M. Morse and H. Feshbach. *Methods of theoretical physics, Part II*. McGraw-Hill, New York, 1953.
- [26] AP Zielinski and Olgierd C Zienkiewicz. Generalized finite element analysis with T-complete boundary solution functions. *International Journal for Numerical Methods in Engineering*, 21(3):509–528, 1985.
- [27] Qing-Hua Qin. Trefftz finite element method and its applications. *Applied Mechanics Review*, 58(1-6):316–337, 2005.
- [28] F dell’Isola, G C Ruta, and R C Batra. A second-order solution of Saint-Venant’s problem for an elastic pretwisted bar using Signorini’s perturbation method. *Journal of elasticity*, 49:113–127, 1997.